

# Session 1A6b

## Antennas and Resonators

<b>Admittance Characteristics of Open Slot Radiators</b>	
<i>G. S. N. Raju (AU College of Engineering, India); Y. V. Narayana (ANITS Engineering College, India);</i>	238
<b>Wide Axial Ratio Bandwidth Circular Polarized Dielectric Resonator Antenna</b>	
<i>R. Chair (University of Mississippi, USA); S. L. S. Yang (City University of Hong Kong, Hong Kong);</i>	
<i>A. A. Kishk (University of Mississippi, USA); K. F. Lee (University of Mississippi, USA); K. M. Luk (City University of Hong Kong, Hong Kong);</i>	239
<b>Radiation <math>Q</math> and Efficiency of Ideal Dipoles inside a Spherical Shield</b>	
<i>J. C.-E. Sten (Technical Research Centre of Finland, Finland); A. Hujanen (Technical Research Centre of Finland, Finland);</i>	240
<b>Theory of Size Reduction of DRA Resonators</b>	
<i>A. A. Kishk (University of Mississippi, USA);</i>	241
<b>Waveform Prediction of a Pulse Communication Link between Antennas Modeled by a Combination of Thin-wires</b>	
<i>F. Sagnard (IETR, INSA, France); G. El-Zein (University of Marne-La-Vallée, France);</i>	242

## Admittance Characteristics of Open Slot Radiators

**G. S. N. Raju and Y. V. Narayana**  
AU College of Engineering, India

The inclined slots cut in the narrow wall of a rectangular waveguide are commonly used for producing horizontally polarized waves. Moreover, slots of resonant length as radiating elements in the array are preferred in most of the applications. But it is not possible to accommodate the slots of resonant length in the narrow wall of standard X-band rectangular waveguide. Hence they are protruded into the broad wall and are analyzed by several Researchers. It is found from the literature and also from our investigations that the protruded pieces of slots into the broad wall lead to undesired polarized components.

In the view of the above facts, a slot of resonant length is accommodated in the present work by increasing only the narrow wall without disturbing broad wall dimensions. The analysis involves plane wave spectrum approach and the admittance characteristics of the slot are obtained. The resultant double integrals are evaluated numerically after testing for convergence.

The arrays of such slots are extremely useful for the design of planar arrays and if the inclination of the slots from broad side is made small, the horizontal polarization is found to be almost maintained.

For the design of large arrays, slots of low conductances are found to be desirable. The low conductances are obtained by controlling width, length, inclination of the slots. The narrow wall dimensions has become an additional parameter for the design of the Arrays in the present work. The admittance data presented is extremely useful for the design of both linear and planar arrays.

## Wide Axial Ratio Bandwidth Circular Polarized Dielectric Resonator Antenna

R. Chair<sup>1</sup>, S. L. S. Yang<sup>2</sup>, A. A. Kishk<sup>1</sup>, K. F. Lee<sup>1</sup>, and K. M. Luk<sup>2</sup>

<sup>1</sup>University of Mississippi, USA

<sup>2</sup>City University of Hong Kong, Hong Kong

Dielectric resonator antenna (DRA) has attracted considerable interest due to its inherent advantages of light weight, small size, low cost, ease of excitation and less conductor loss compared to patch antennas. DRAs can be made with different materials with a wide range of permittivities. DRAs have been designed to provide a variety of performance characteristics, such as wide band, dual band and circular polarization. In particular, with suitable design, the impedance bandwidth of a DRA element can attain 30% or more.

In [1], a 45° rotated rectangular DRA with permittivity 10.8 is excited by a narrow rectangular slot. It radiates circularly polarized waves with 6.6% axial ratio (AR) bandwidth. Wider AR bandwidth (in the range of 10% – 20%) designs reported in the literature usually involve either complex excitation or in the array form [2, 3].

In this paper, using a stair case structure, a simple aperture coupled DRA with wide AR bandwidth is presented. The 45° rotated stair DRA is excited by a microstrip line through a narrow rectangular slot. Using rectangular DR shapes with a length to width ratio of 1.9, two degenerate orthogonal modes are excited, generating circular polarization. The measured results show an impedance matching impedance bandwidth ( $S_{11} < -10$  dB) of 36.6% with  $\epsilon_r = 12$  and a measured AR bandwidth (AR < 3-dB) of 10.6%, with stable broad-side radiation patterns. The AR bandwidth of the proposed simple DRA is comparable to more complicated designs reported in the literature. Simulation (from HFSS) and measured results show good agreement.

### REFERENCES

1. Oliver, M. B., Y. M. M. Antar, R. K. Mongia, and A. Ittipiboon, "Circularly polarized rectangular dielectric resonator antenna," *Electron. Lett.*, Vol. 31, No. 6, 418–419, Mar. 1995.
2. Haneishi, M. and H. Takazawa, "Broadband circularly polarized planar array composed of a pair of dielectric resonator antennas," *Electron. Lett.*, Vol. 21, No. 10, 437–438, May 1985.
3. Pang, K. K., H. Y. Lo, K. W. Leung, K. M. Luk, and E. K. N. Yung, "Circularly polarized dielectric resonator antenna subarrays," *Microwave and Optical Tech. Lett.*, Vol. 27, No. 6, 377–379, Dec. 2000.

## Radiation $Q$ and Efficiency of Ideal Dipoles inside a Spherical Shield

J. C.-E. Sten and A. Hujanen

Technical Research Centre of Finland, Finland

In this paper an account is given of the effects of a semitransparent (low-loss) dielectric or magnetic shield on the operation of electrically small antennas. An obvious motivation for the work is that mobile terminal antennas are nowadays often embedded within the equipment. Two parameters form our principal interest here; 1: the quality factor,  $Q$ , computed from the ratio between the energy stored and the power accepted by the antenna, and 2: the radiation efficiency,  $\eta$ , or the proportion of radiated power to net power delivered to the antenna. Our approach is theoretical; we describe a method for calculating these quantities for azimuthally symmetric electric (TM) and magnetic (TE) multipoles surrounded by a semitransparent spherical shield of variable thickness, dielectric and magnetic constants with losses. Thus, a boundary value problem for the electromagnetic fields is formed. For its solution, a matrix method is applied to relate the transverse field components at each pair of adjacent interfaces. The method is hereupon applied to the case of a shield consisting of a single homogeneous layer. The  $Q$  and efficiency for such a structure are determined by computing numerically the energy stored in the near field of the multipole as well as the power radiated and dissipated in the shield. The performances of TM and TE multipole radiators are compared as a function of frequency. Hence, it is seen that even a very thin layer of a lossy dielectric considerably degrades the radiation efficiency at low frequencies, however, more severely for electric dipoles than for magnetic ones. Therefore, the electric dipole has a lower radiation  $Q$  than its magnetic counterpart. However, with a growing frequency the differences between the two types of dipoles are seen to balance. Low-frequency series expansions as well as high-frequency asymptotic expansions of the efficiency are given to elucidate the importance of the material parameters of the shield. We also derive some closed-form expressions for the dielectric permittivity of the shield and its outer and inner radii, which minimises the  $Q$ .

## Theory of Size Reduction of DRA Resonators

A. A. Kishk

University of Mississippi, USA

Dielectric resonator antennas have found increase interest because of their many advantages as efficient radiators. In the X-band and higher the antenna size is very small, but at low frequencies the antennas size may not be suitable and one has to use very high dielectric constant in order to reduce the size, but the bandwidth decreases dramatically because of the high quality factor. Since for mobile personal communications, the radiation patterns are not very critical. Another method to reduce the antenna size with wide bandwidth is desired. Here we propose a method of size reduction that was used successfully with microstrip patches [1]. The method depends on the nature of the mode excited within the full size resonator. It is well known that a perfect electric conductor (PEC) passing by a plane with zero tangential electric fields or only orthogonal electric field can be replaced with a PEC plate without disturbing the original field distribution and thus reducing the space by half and keeping the same resonant frequency of the antenna. This is corresponding to reducing the antenna size to half. This is actually what is used with the DRA antennas above a PEC. If the mode has a plane of symmetry with respect to the geometry and excitation and parallel to the E-plane of the antenna, the electric fields on this plane will be laying along the plane and the magnetic fields will be orthogonal to this plane. This plane could be replaced by a perfect magnetic conductor (PMC) without disturbing the field distribution and thus keeping the same resonant frequency and reducing the antenna size to half. However, there is no natural PMC to be used. Therefore, the reduction of the size using this plane needs to be considered carefully. Although, artificial magnetic conductors can be realized, this will not serve the purpose of size reduction because these materials to be useful its size might be larger than the size of the antenna itself.

The fields inside the dielectric resonator of the high dielectric materials see the dielectric surface as nearly magnetic conductor. Such an assumption is by itself is a useful argument that makes us believed that this plane exists naturally if the dielectric materials of one half are removed. Of course, such an assumption becomes better as the dielectric constant increases.

Demonstration of this argument will be presented by several DRA designs that keep the bandwidth of the full size DRA even after the size reduction that could be more than 75% of the full size DRA.

### REFERENCES

1. Kishk, A. A., et. al., *IEEE Transactions on Antennas and Propagation*, Vol. 52, No. 1, January 2004.

# Waveform Prediction of a Pulse Communication Link between Antennas Modeled by a Combination of Thin-wires

F. Sagnard<sup>1</sup> and G. El-Zein<sup>2</sup>

<sup>1</sup>IETR, INSA, France

<sup>2</sup>University of Marne-La-Vallée, France

**Abstract**—In the context of the development of the emerging Ultra-Wide Band (UWB) technology, the modelling and the analysis of the transient waveforms radiated and received in a communication link are proposed. The modelling developed, based on analytical expressions, allows to consider combinations of thin-wire elements to represent conductive antennas with a 2D or 3D geometry. The propagation channel has been modelled by the presence of a dielectric material in air. Detailed parametric studies have been performed, and optimization of the antenna characteristics has been addressed. This work appears as a synthesis and an extension of previous studies.

## 1. Introduction

In recent years, the Ultra-Wide Band (UWB) technology appears as an attractive solution for technical improvements in conventional narrow band wireless communication systems. Such a technology relies initially on the transmission of a series of baseband modulated (in amplitude or phase) short pulses (less than 1 ns) with a low duty cycle. Such signals have an energy which is spread thinly across the entire broadband spectrum (greater than 500 MHz with a fractional bandwidth of more than 20%), thus allowing the UWB technology to coexist with other wireless systems without licence. This technology offers several advantages such as: transmission at a high bit rate, low cost, low probabilities of interception and detection, separation of multipath... Therefore, several applications are being implemented including communications, networking, radar (GPR, vehicular, surveillance) imaging (medical, through-wall, construction materials, security, GPR), and measurement devices (sensors, positioning). Currently, the FCC has regulated UWB power levels emitted by defining a spectral mask in the -10 dB bandwidth between 3.1 and 10.6 GHz in order to limit interferences with existent licensed wireless systems (WLANs, GPS). Efforts are under way by the IEEE community for standardizing the use of UWB systems in indoor (home and office) multimedia transmissions.

Because of the very wide frequency band of the transmitted signal, novel studies concerning the modelling and the characterization of the propagation channel and of the antennas have to be achieved; it appears that in such a case the studies are best performed in the time domain. Therefore, we have focused our studies on the modelling and on the parameter analysis of the physical phenomena involved in the transient radiation, propagation and reception of a pulse signal in a simplified multipath propagation channel including a dielectric sample in air. The modelling tool uses extended analytical expressions, in the transmission and reception configurations, to describe the responses of conductive antennas made of a combination of infinitely and loaded linear thin-wire elements, representing several 2D or 3D antenna geometries (V-dipole, bow-tie, butterfly, TEM horn...). Such an original tool which includes extended developments of previous work allows to highlight the pulse-shaping process in the spatio-temporal domain [1, 3, 5].

## 2. Transient Responses of Thin-wire Elements

The basic transmission link is composed of single transmitting and receiving antennas separated by a distance  $d$  in the far-field zone of each other over the operating frequency bandwidth; the major component of the radiating field  $E_\theta(r, \theta, \phi)$  is oriented along the direction  $\vec{\theta}$ . The antennas do not necessarily face each other and can be tilted. The transmitting antenna is positioned at the origin 0, and two angles  $\beta$  and  $\phi$  define the position of each wire element to axis  $Oz$  and axis  $Ox$  respectively. The propagation channel is modelled by the presence of a dielectric material with large dimensions which has been placed in the air between both antennas; thus, diffraction does not occur at the edges. The link modelled is presented in Figure 1 with the parameters associated with the frequency domain to highlight the presence of the several frequency-dependent impedances involved in the input and output circuits.

The modelling approaches described in this section concern in transmission symmetric straight dipoles  $(-L, L)$ , and in reception symmetric V-dipoles  $(-L, L)$ . In transmission, as the expressions allow to distinguish the radiated components of the electric field issued from each monopole, the extension of the modelling

to a V-dipole can be easily deduced by tilting each arm. In reception, it appears more natural to model the physical phenomena involved in each arm individually. From the analytical expressions developed, other dipole orientations can be considered [2].

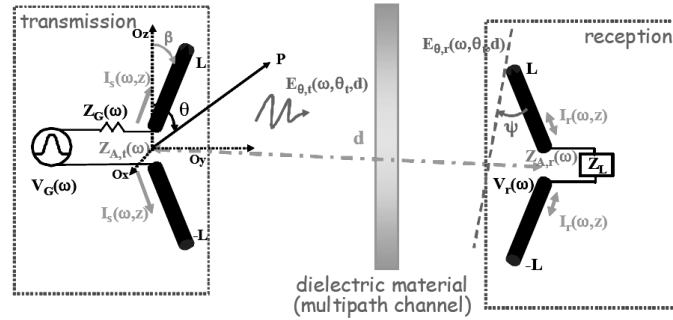


Figure 1: Geometry of the link between two V-dipoles with their parameters in the frequency domain.

### 2.1. Transmission Configuration

The straight dipole  $(-L, L)$  aligned with axis  $Oz$  is supposed to be excited at the feed point  $z = 0$  by an impulse current which has generally the shape of the Gaussian function or one of its successive derivatives. The  $p$ -th derivative  $g(t)$  of the Gaussian function is expressed by:

$$g^{(p)}(t) = \frac{d^p}{dt^p} (A_0 e^{-\frac{t}{\tau}}) \quad (1)$$

where  $\tau$  represents the characteristic time of the pulse, and  $A_0$  its amplitude. The duration  $w$  of each signal has been defined as the time interval centered on the pulse shape and containing 99% of the total energy of the pulse. For example,  $w = 3.3\tau$  for  $p = 0$ ,  $w = 4.08\tau$  for  $p = 1$ , and  $w = 4.5\tau$  for  $p = 2$ . In general,  $\tau$  has been set in order to fit a number  $n$  not necessarily an integer of pulse durations in each arm length of the dipole. Thus, we defined the reference time  $\tau_a = L/c = nw$ , where  $c$  represents the velocity in the air.

In the case of an infinitely conductive dipole, the initial current wave  $I_s(t - |z/c|)$  which propagates along both arms undergoes a total reflection (with a coefficient -1) as it reaches both terminations  $z = L$  and  $z = -L$ , and a partial reflection at the feed point (denoted  $\rho$ ). The back and forth propagation process continues until the traveling current undergoes a complete attenuation [1, 3]. Such a ringing effect produces narrow frequency radiated waveforms, and usually the objective is to reduce it as much as possible. In general, the dipole radiation is produced at the positions  $z = 0$ ,  $z = L$ , and  $z = -L$ . In the far-field zone, the main electric field component  $E_\theta(r, \theta, t)$  in the spherical coordinates  $(r, \theta)$  is expressed as follows [3]:

$$E_\theta(r, \theta, t) = \frac{\eta_0}{4\pi r} \left[ \sum_{i=1}^{\infty} \Gamma_i \frac{\sin \theta}{(1 - \cos \theta)} \{I_s(t - r/c - b_i) - I_s(t - r/c - (L/c)(1 - \cos \theta) - b_i)\} + \Gamma_i \frac{\sin \theta}{(1 + \cos \theta)} \{I_s(t - r/c - c_i) - I_s(t - r/c - (L/c)(1 + \cos \theta) - c_i)\} \right] \quad (2)$$

$$b_i = \begin{cases} (L/c)(i - 1 + \cos \theta) & i \text{ even} \\ (L/c)(i - 1) & i \text{ odd} \end{cases} \quad c_i = \begin{cases} (L/c)(i - 1 - \cos \theta) & i \text{ even} \\ (L/c)(i - 1) & i \text{ odd} \end{cases} \quad (3)$$

$$\Gamma_i = \begin{cases} (-1)^{i/2} \rho^{(i/2-1)} & i \text{ even} \\ (-\rho)^{(i-1)/2} & i \text{ odd} \end{cases} \quad (4)$$

where  $\eta_0$  represents the wave impedance in the vacuum. In relation (2), we can distinguish the contribution of both arms  $(0, L)$  and  $(0, -L)$  of the dipole to the radiated field induced by upward and downward propagating current components respectively: as the factor  $\sin \theta / (1 - \cos \theta)$  corresponds to the upper arm, the factor  $\sin \theta / (1 + \cos \theta)$  is associated with the lower arm. We notice that the total electric field radiated is built from differentiated delayed current components that express the time derivative of the current in each arm if the two components are separated by a delay  $\Delta t = \tau_a(1 - \cos \theta) \geq \omega$  and  $\Delta t = \tau_a(1 + \cos \theta) \geq \omega$ . Also, we remark that the radiation of the lower arm is the same as the radiation of the upper arm when changing the observation angle  $\theta$  to its complementary value  $\pi - \theta$ . Such a modeling has been compared to a numerical one based on the FIT, and the results agree satisfactorily.

In the case of a Wu and King (WK) loaded dipole, a distributed complex impedance along each arm length of the dipole is expressed by [4]:

$$Z(z, \omega) = \frac{1}{Y(z, \omega)} = r(0, \omega) \left( \frac{L}{L - |z|} \right) \left( 1 - j \frac{k_0}{L} \right) \quad (5)$$

where  $k_0$  is the wave number in the vacuum, and  $r(0, \omega) = \frac{\eta_0 \psi}{2\pi}$  the impedance at the feed-point  $z = 0$  of the dipole.  $\psi$  is a function of the frequency, and  $\eta_0$  the impedance of the free space. For the sake of simplicity, the parameter  $\psi$  is replaced by its mean value over the given frequency bandwidth considered. The expression of the transient radiated electric field given by Samaddar et al. extended to consider the presence of an impedance associated with the input circuit is given by [5, 6]:

$$E_\theta(r, \theta, t) = \frac{1}{r\psi \sin^2 \theta} \frac{\tau_a}{\tau_t} \left[ \begin{aligned} & \sin^2 \theta (V_G(t^*) - \frac{1}{\tau_t} \int_0^\infty V_G(t^* - t') e^{-t'/\tau_t} dt') \\ & - \frac{(1 + \cos^2 \theta)}{\tau_t} \int_0^\infty V_G(t^* - t') e^{-t'/\tau_t} dt' \\ & + \frac{(1 + \cos \theta)^2}{2\tau_t} \int_0^\infty V_G(t_1 - t') e^{-t'/\tau_t} dt' \\ & + \frac{(1 - \cos \theta)^2}{2\tau_t} \int_0^\infty V_G(t_2 - t') e^{-t'/\tau_t} dt' \end{aligned} \right] \quad (6)$$

where:  $t^* = t - r/c$ ;  $t_1 = t^* - \tau_a(1 - \cos \theta)$ ;  $t_2 = t^* - \tau_a(1 + \cos \theta)$ . Also,  $\tau_t = C_g \tau_a$  with  $C_g = 1 + 2\pi Z_G / (\eta_0 \psi)$ .  $Z_G$  is a constant representing the mean value of the impedance associated with the input circuit in the frequency bandwidth of the excitation signal. If  $Z_G = 0$ , we have  $\tau_t = \tau_a$ .

## 2.2. Reception Configuration

A dipole antenna  $(-L, L)$  such as presented in Figure 1 is supposed to be excited at the upper arm by a transient electric plane wavefront with an oblique incidence angle  $\psi$  relative to the direction of the antenna. Two cases can be distinguished depending if a straight or a V-dipole is considered: in the case of a straight dipole, as the upper arm is first excited at its top, the lower arm is first excited at the position  $z = 0$ . In the case of a V-dipole, both upper and lower arms are first excited at their top. The analytical developments presented in this paper concern a monopole  $(0, L)$  initially aligned with axis  $O_z$ . If the monopole is tilted with an angle  $\beta$  relative to axis  $O_z$  the expressions remain valid, and the case of a monopole  $(0, -L)$  tilted with an angle  $-\beta$  relative to axis  $O_z$  can be deduced from the expression of the upper monopole by adding an additional delay  $\tau'_D = L \sin \psi / c$  and changing the incidence angle  $\psi$  by its complementary value  $\pi - \psi$ . The excitation signal  $E_\theta(\theta_r, t)$ , which is supposed to be issued from a transmitting antenna of the same kind, interacts with a given monopole  $(0, L)$  and produces at each point of the element of abscissa  $z'$  an induced current  $dI'(z, t; z')$ . This current propagates from each excitation point  $z'$  in two opposite directions [2]. A time delay  $\tau_D$  is assigned to each discrete source to represent the arrival time of the oblique plane wave front with incidence  $\psi$  on the antenna:

$$\tau_D = (L - z') \sin \psi / c \quad (7)$$

$$dI(z, t; z') = \left\{ \begin{aligned} & dI'(z', t - (z - z')/c - \tau_D) \cos \psi \cdot U(z - z') \\ & + dI'(z', t - (z + z')/c - \tau_D) \cos \psi \cdot U(z' - z) \end{aligned} \right\} [U(z) - U(z - L)] \quad (8)$$

where  $U$  is the Heaviside unit-step function. Each local current component mentioned in relation (8) writes as follows:

$$dI'(z', t) = Y(z') E(z', t - \tau_D) = 1/Z(z') E(z', t - (L - z') \sin \psi / c) \quad (9)$$

where  $Z(z')$  represents the impedance which can vary along the antenna.

In the case of a uniform infinitely conductive antenna, we have extended previous developpement in order to consider the total current component distributed along the antenna arms for an oblique incidence. For the sake of simplicity the formulation concerning the upper monopole  $(0, L)$  does not include the ringing elect issued from total and partial reflections at the top end and the feed point respectively:

$$\begin{aligned} I_{upper}(z, t) &= \frac{c \cos \psi}{1 + \sin \psi} \{ \xi(t - (L - z) \sin \psi / c) - \xi(t - z/c - L \sin \psi / c) \} \\ &+ \frac{c \cos \psi}{-1 + \sin \psi} \{ \xi(t - (z - L)/c) - \xi(t + (z - L) \sin \psi / c) \} \end{aligned} \quad (10)$$

And  $\xi(t) = \int_0^t E(t') dt'$ . At the position  $z = 0$ , the current detected becomes:

$$I_{upper}(0, t) = -\frac{c \cos \psi}{1 + \sin \psi} \xi(t - L \sin \psi / c) - \frac{c \cos \psi}{1 - \sin \psi} \xi(t - L/c) + \frac{2c}{\cos \psi} \xi(t - L \sin \psi / c) \quad (11)$$

In the case of a WK loaded dipole, we have expressed the current generated by each local source along the upper monopole  $(0, L)$  as follows:

$$dI'(z, t; z') = Y(z', t) \otimes E(z', t - (L - z') \sin \psi / c) \cos \psi \quad (12)$$

where  $\otimes$  denotes the time convolution product. Then, replacing the local current  $dI'(z, t; z')$  in relation (8),

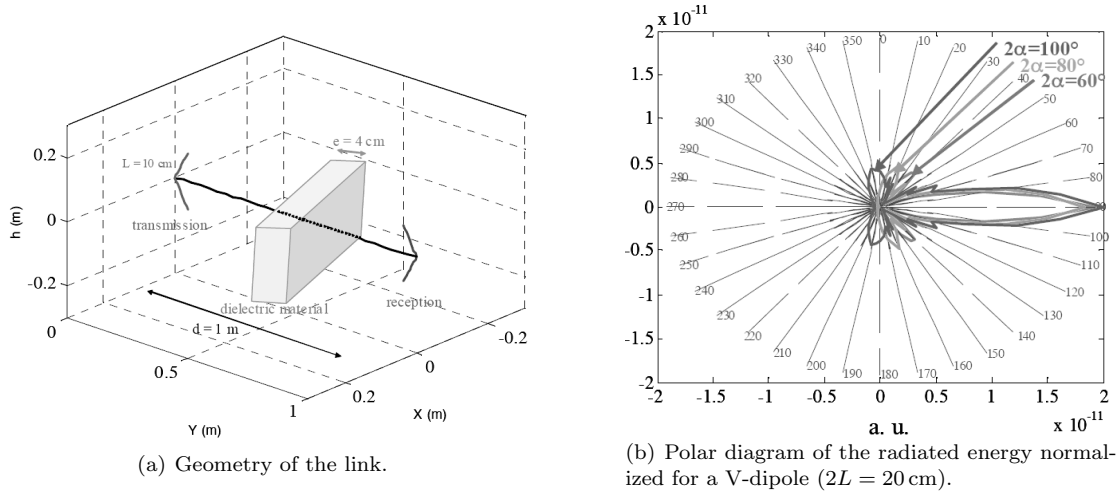


Figure 2: (a) Geometry of the link simulated involving two V-dipoles in the far-field and a single-layer dielectric material; (b) Polar diagram of the radiated power of a uniform V-dipole for several aperture angles.

we obtain an additional component  $I'_{upper}(z, t)$  which superimposes on the current component  $I_{upper}(z, t)$  associated with the uniform monopole. It is defined as follows:

$$I'_{upper}(z, t) = I'_{top}(z, t) + I'_{bottom}(z, t) \quad (13)$$

$$\text{with: } I'_{top}(z, t) = \frac{c \cos \psi}{1 + \sin \psi} \left\{ \begin{array}{l} z\xi(t + (z - L) \sin \psi/c) \\ + \frac{1}{L} \frac{c}{1 + \sin \psi} [\zeta(t + (z - L) \sin \psi/c) - \zeta(t - z/c - L \sin \psi/c)] \end{array} \right\} \quad (14)$$

$$I'_{bottom}(z, t) = -\frac{1}{L} \frac{c \cos \psi}{-1 + \sin \psi} \left\{ \begin{array}{l} L\xi(t + (z - L)/c) - z\xi(t + z(z - L) \sin \psi/c) \\ + \frac{1}{L} \frac{c}{-1 + \sin \psi} [\zeta(t + (z - L)/c) - \zeta(t + z/c - L \sin \psi/c)] \end{array} \right\} \quad (15)$$

And  $\zeta(t) = \int_0^t \xi(t') dt'$ . Then the total current component without reflection at the feed-point is given by:

$$I_{WK,upper}(z, t) = \frac{1}{r(0)} (I_{upper}(z, t) + I'_{upper}(z, t)) \otimes e^{-t/\tau_a} \quad (16)$$

At the position  $z = 0$ , the current received by the detector is:

$$I_{WK,upper}(0, t) = \frac{1}{r(0)} (I_{upper}(0, t) + I'_{upper}(0, t)) \otimes e^{-t/\tau_a} \quad (17)$$

Relation (16) appears as an extended version of the expression given by Samaddar et al., [5], as it allows to study the current distribution along each arm of a dipole and not only at the position  $z = 0$ .

### 3. Simulation Results

As an illustration of the modelling presented above, we have considered in transmission and reception two identical symmetric V-dipoles formed of two thin-wire elements with length  $L = 10$  cm and characterized by an aperture angle  $2\alpha = 120^\circ$  ( $\beta = 30^\circ$ ) as presented in Figure 2(a). The dipoles which face each other have been fixed in each other far-field at a distance  $d = 1$  m. The equivalent impedances at the feed-point in transmission and reception have been estimated to  $600 \Omega$ . The excitation voltage in transmission is assumed to have the shape of the first derivative of the Gaussian function; the reference characteristic time  $\tau$  has been fixed to 41.25 ps (which corresponds to the duration  $\omega = 0.17$  ns), so that 2 pulses ( $n = 2$ ) fit in each arm length  $L$ . The propagation channel is represented here by a single-layer dispersive dielectric material with thickness  $e = 4$  cm; in the modelling, any multi-layer dielectric sample with a plane surface can be considered. In transmission, we have studied the influence of the aperture angle  $2\alpha$ , and the pulse duration (by the means of  $n$ ) on the focalization of the electromagnetic energy radiated in the direction  $\theta = 90^\circ$ . Some results associated with a uniform V-dipole are presented in Figure 2(b) for three angles  $2\alpha = 60^\circ, 80^\circ, 100^\circ$ ; they show that a focalization in the direction  $\theta = 90^\circ$  is obtained for  $n = 2.9, 1.7$  and  $0.9$  pulses in a arm length  $L = 10$  cm (for  $2\alpha = 120^\circ$ , we have found that  $n = 0.8$ ). The polar diagram highlights that a narrower focalization is obtained for the lowest aperture angle  $2\alpha$ . Moreover, the spatio-temporal waveforms radiated in the far-field zone by a uniform (with

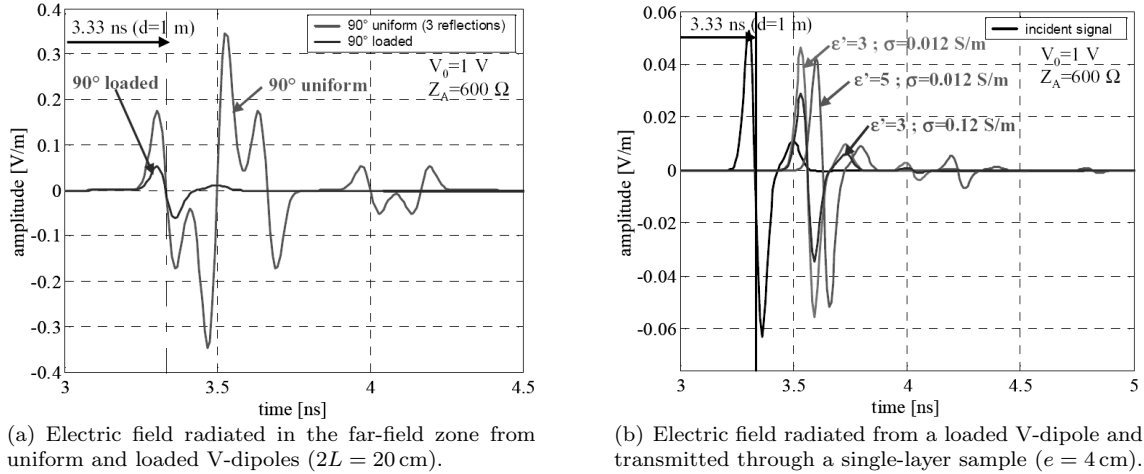


Figure 3: (a) Waveforms radiated by uniform and loaded V-dipoles; (b) Resulting waveforms radiated by a loaded V-dipole and transmitted through a single-layer dielectric sample ( $e = 4$  cm).

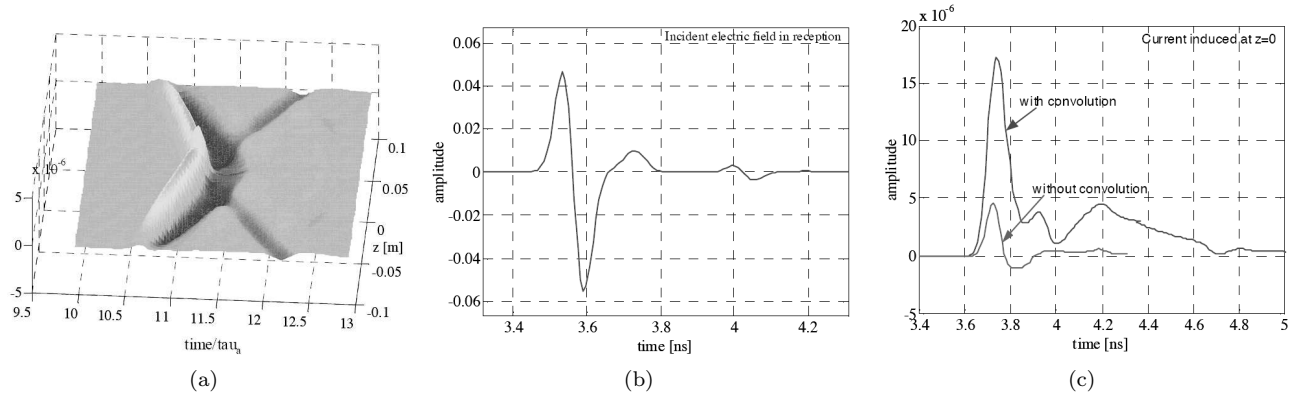


Figure 4: (a) 3D current distribution along the V-dipole ( $2\alpha = 120^\circ$ ,  $L = 10$  cm, incidence  $\varphi = 0^\circ$  so  $\Psi = 30^\circ$ ); (b) Current distribution induced in a loaded V-dipole in the reception configuration considering the incident wavefront (a); (c) Detected current at the position  $z=0$ .

3 reflections) and a loaded V-dipole of the same dimensions have been compared; the plots of Figure 3a which consider the direction  $\theta = 90^\circ$  show that as the uniform V-dipole gives a distorted version of the excitation signal with a ringing phenomenon, the loaded V-dipole generates an attenuated and a slightly distorted version of the initial pulse. Then, we have studied the transmission of the signal radiated by the loaded dipole under the incidence angle  $\theta_i = 0^\circ$  and through a single layer material considering the following dielectric properties: (1)  $\epsilon' = 3$ ,  $\sigma = 0.012$  S $\cdot$  m $^{-1}$ , (2)  $\epsilon' = 3$ ,  $\sigma = 0.12$  S $\cdot$  m $^{-1}$ , and (3)  $\epsilon' = 5$ ,  $\sigma = 0.012$  S $\cdot$  m $^{-1}$ . The resulted waveforms can be visualized in Figure 3(b). The corresponding ratios of the energy transmitted to the energy of the incident signal are respectively 77.7%, 30.3%, and 68.5%. So, these results highlight the strong attenuation effect introduced by the losses produced inside the material. Afterwards, considering the signal transmitted through the sample with the dielectric properties  $\epsilon' = 3$ ,  $\sigma = 0.012$  S $\cdot$  m $^{-1}$  (see Figure 4(b)), we have computed the current distribution in a loaded V-dipole ( $\beta = 30^\circ$ ). The 3D plot of Figure 4(a) shows the induced current before executing the convolution product with the term  $e^{-t/\tau_n}$  and mentioned in relation (16). The current at the position  $z = 0$  is visualized in Figure 4(c) before and after the convolution operation. We remark that such an operation smooths the signal.

#### 4. Conclusion

In this paper, the modelling of a communication link involving two transmitting and receiving antennas in the time domain has been revisited. The modelling, based on analytical expressions, allows to consider several

conductive antennas which can be represented by a simplified model using a combination of non interacting thin-wire elements. Further developments have been made mainly in the reception configuration in order to consider the interaction of a uniform or a loaded Wu and King dipole which are supposed to be illuminated by an oblique plane wavefront. At present, the propagation channel has been represented by the presence of a multi-layer dielectric dispersive material which produces multipath induced by the multiple reflections occurring in its thickness. Statistical models of propagation channel, such as the Turin approach, associated in a given environment can be planned. Samples of the parametric studies made have been presented in the case of a communication link involving two transmitting and receiving V-dipoles. We have particularly analyzed the case of a WK V-dipole as its better represents an UWB band as the ringing effect of the current has been eliminated by a distributed absorption along each arm. The realization of a graphical interface will make easier more parametric studies to thoroughly analyzed the link budget in a given configuration. Moreover, optimization of the link will be addressed.

## REFERENCES

1. Bantin, C. C., "Pulsed communications link between dipoles," *IEEE Antennas and Propagat. Magazine*, Vol. 44, No. 5, 75–82, October 2002.
2. Sagnard, F., "Propagation and radiation studies for the development of the future communication systems," Habilitation à Diriger des Recherches, University of Marne-La-Vallée, France, 23 March, 2005.
3. Martin, R. G. and J. A. Morente, "An approximate analysis of transient radiation from linear antennas," *Int. Journal Electronics*, Vol. 61, No. 3, 343–353, 1988.
4. Wu, T. T. and R. W. P. King, "The cylindrical antenna with non-recting resistive loading," *IEEE Trans. Antennas Propagat.*, Vol. 13, 369–373, May 1965.
5. Samaddar, S. N. and E. L. Mokole, "Transient behaviour of radiated and received fields associated with a resistively loaded dipole," *Ultra-Wideband Short Pulse Electromagnetics 4*, Herman et al., Kluwer, 165–179, 1999.
6. Sagnard, F. and C. Vignat, "Extension of the analytical modelling of resistive loaded thin-wire antennas to Gaussian derivatives excitations," *Microwave Optical Technology Letters*, Vol. 47, No. 6, 548–553, December 2005.

